

Importance of Rotational Losses in Rotating Machines and Transformers

A.J. Moses

There are increasing calls for a standard specification for the measurement of rotational losses in electrical steels and amorphous magnetic materials. However, the question still remains as to whether rotational losses are sufficiently important in practice to merit the implementation of a special standard. This paper explains what rotational magnetization is and how the losses occur. It then gives a brief explanation of the measurement difficulties encountered. Regions of transformers and rotating machine cores where rotational flux occur are illustrated and an estimate of the resulting rotational losses is made. It is shown that the proportion of rotational loss in transformers is not generally high, whereas in motors it can amount to more than 50% of the total core loss. The results indicate that rotational loss is of sufficient importance in motors to merit the establishment of standardized methods of measuring it in magnetic materials.

1 Introduction

CORE losses in laminated magnetic cores consume over 3% of all electricity generated; consequently, producers of electrical steels and the manufacturers of electrical machines and transformers are attempting to cut these losses by developing new magnetic materials and using them more effectively. The core losses in electrical machines may be regarded as taking place as a result of two main mechanisms. The first is when flux changes cyclically in magnitude and direction in the plane of a lamination, but does not vary in angular direction. This gives rise to alternating power loss. The second occurs when the magnetic field and flux rotate in the plane of a lamination and give rise to rotational losses. It is well known that, at most magnetization levels, the loss due to rotational flux is much higher than that due to alternating flux.

Rotational flux occurs in the corner joints of three-phase laminated transformer cores and behind the teeth of ac rotating machine stator cores. The magnetization in these regions is very complex and is completely different from the condition under which electrical steel laminations are tested for quality control or grading. The well-known Epstein test[1] is used to measure the loss of 30- by 3-cm strips of electric steel magnet-

A.J. Moses, Wolfson Centre for Magnetics Technology, School of Electrical, Electronic and Systems Engineering, University of Wales College of Cardiff, Cardiff, Wales, UK.

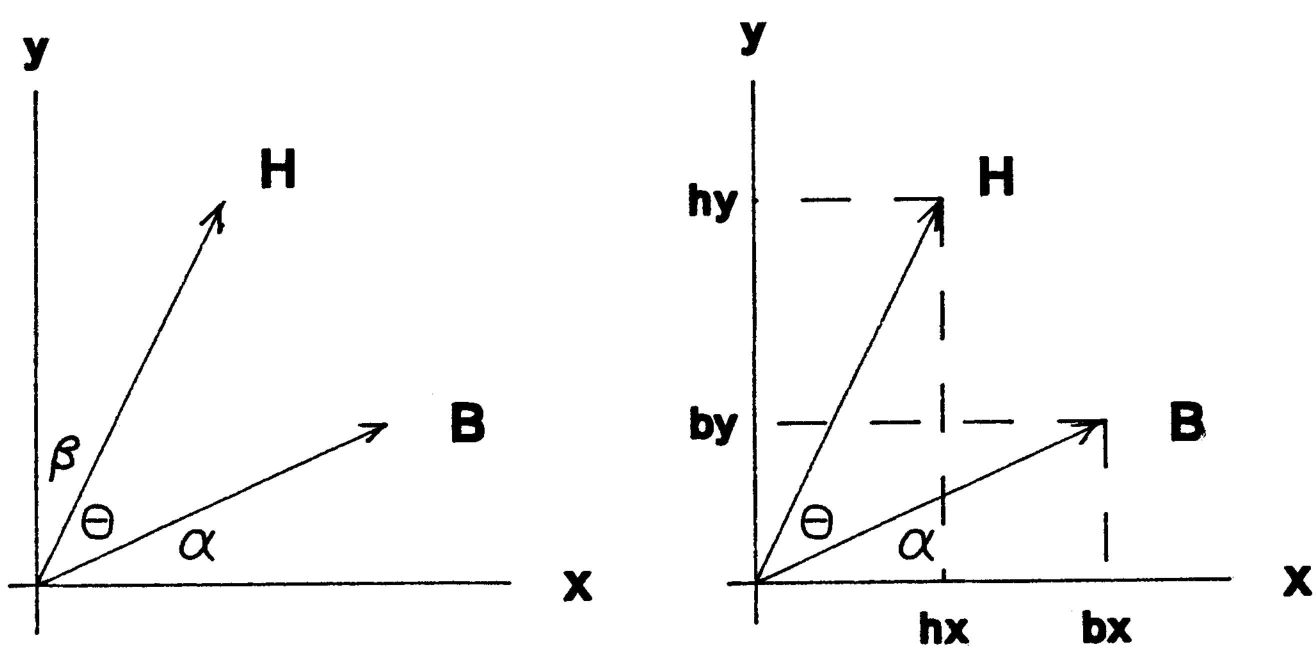

Fig. 1 Representation of field (H) and flux density (B) vectors in the plane of a sheet. **(a)** Slow magnetization conditions. **(b)** Analysis of rotating components into orthogonal components.

ized under pure sine wave magnetization conditions. The steel is graded and sold on the basis of the results of this test, and machine performance and efficiency calculations are often based on these data. Rotational magnetization that might occur in the final application is not taken into consideration. Even as long ago as 1970, when the capitalized cost of iron losses was only around £75/kW (approximately \$125) in the UK, the importance of rotational loss in large machines was well recognized.[2] It is now becoming increasingly important to know to what extent the performance of a magnetic material under rotational flux conditions will affect the efficiency of a motor or transformer.

The aim of this article is to answer some questions, which will help show the importance of rotational losses in power devices. The article first discusses what rotational flux is and how it can be measured. Next, examples of its occurrence in rotating machines and transformers are given, and an estimate of the contribution of rotational losses to their total core losses is made to show its importance in machine design.

2 Basic Theory of Rotational Magnetization

Consider a magnetic field, H_R, slowly rotating in the plane of a sheet of magnetic material. The flux density, B_R, will rotate in a similar manner, ideally lagging the field by a constant angle, θ, in space. At any instant, a torque, T, will be exerted on the material given by:

$$T = B_R H_R \sin\theta \quad [1]$$

At low speeds of rotation, this torque can be measured (for instance using a torque magnetometer), and it gives rise to a rotational hysteresis loss, P_{RH}, given by:

$$P_{RH} = \int_0^{2\pi} B_R H_R \sin\theta \, d\alpha \quad [2]$$

where α is the angle H_R makes with a reference direction. This is illustrated schematically in Fig. 1(a). It is assumed that in this process no eddy currents occur so the loss is analogous to the hysteresis loss that occurs under ac magnetization. Figure 2 (based on Ref 3) illustrates the manner in which the surface domain structure of a (100) [100] single crystal of 3% silicon iron changes during half a cycle of such magnetization. Here, the rotating field, H_R, is constant in magnitude, although the flux density will vary in magnitude as the field rotates. At low fields, rotational loss arises due to domain wall motion. However, if the field is increased, the number of walls decreases, and as will be seen later, the loss will drop as saturation is approached, unlike under alternating magnetization conditions.

In practice, it is rare for a material to be subjected to pure alternating flux, and many attempts have been made to predict the losses under these conditions. From Eq 2, the loss per cycle is simply $2\pi B_R H_R \sin\theta$ for an ideal isotropic material when B_R, H_R, and θ remain constant. Several empirical relationships have been developed to try to predict rotational hysteresis loss that occurs in real materials. One relationship that yields quite good practical agreement is:[4]

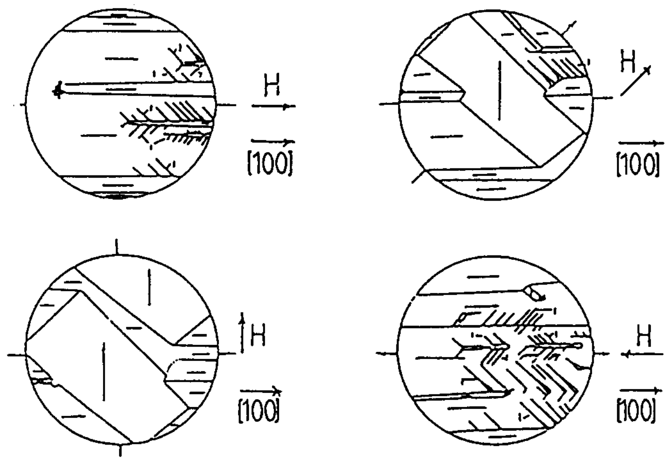

Fig. 2 Representation of domain movement under the influence of a rotating field in a (100) [001] crystal of silicon iron.

$$P_{RH} = P_X\left[\frac{B_X}{B_S} - \left(\frac{B_Y}{B_S}\right)^2\right] + P_Y\left[\frac{B_Y}{B_S} - \left(\frac{B_X}{B_S}\right)^2\right] \quad [3]$$

where P_X is the hysteresis loss on saturation along the X axis; P_Y is the hysteresis loss on saturation along the Y axis; B_X is the component of rotational flux density along the X direction; B_Y is the component of rotational flux density along the Y direction; and B_S is the saturation magnetization.

The equation gives reasonable agreement for $B_X \neq B_Y$, but it does not predict the high increase that occurs around 0.7 B_S or the peak at around 0.8 B_S in real materials.

The ratio of rotational hysteresis to hysteresis under ac magnetization has been predicted from consideration of the magnetization process.[5] The theory predicts that the ratio should be 2:1 in any plane having two equivalent cubic crystal easy directions at right angles (*e.g.*, (100) [100] oriented silicon iron). This agrees quite well with experiment (see Fig. 7). Just as under ac magnetization, when the rate of change of H_R increases, eddy currents are induced and the losses increase.

In isotropic materials, the linear relationship between the vectors of magnetic induction B and of alternating magnetic field strength H is given by use of a scalar permeability, μ. When losses are taken into account, μ becomes a complex number, because B lags H in time. This can be extended to the case of a rotating field[5] by introducing a tensor permeability. In isotropic material, this tensor $\bar{\mu}_{iso}$ can be given by the product of a rotating matrix and a scalar μ as:

$$\bar{\mu}_{iso} = \mu \begin{pmatrix} \cos\theta & \sin\theta \\ -\sin\theta & \cos\theta \end{pmatrix} \quad [4]$$

If the material is isotropic, θ will change during the cycle and a diagonal matrix as below can be used:

$$\bar{\mu}_{aniso} = \begin{pmatrix} \mu_x & 0 \\ 0 & \mu_y \end{pmatrix} \quad [5]$$

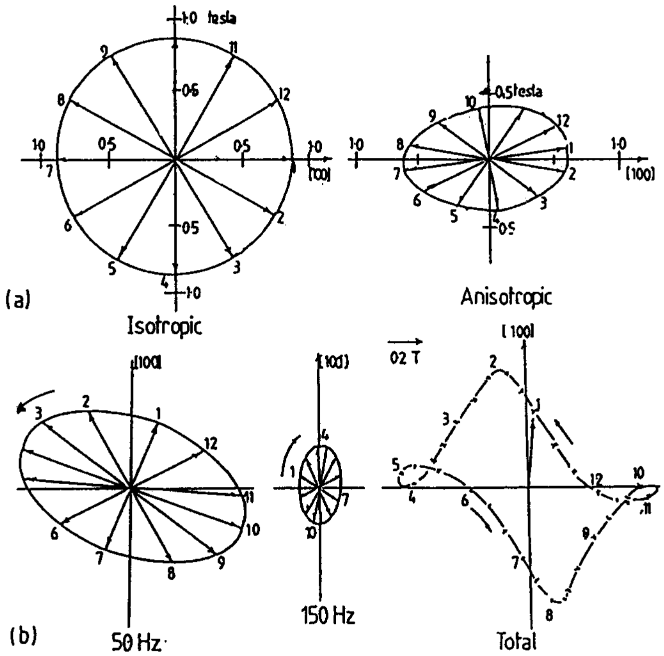

Fig. 3 Schematic of rotational flux density as rotating vectors in various conditions. (a) Isotropic material pure rotational flux and elliptical locus in anisotropic material. (b) Harmonic components of rotating flux and their resultant.

To describe the loss during the rotational magnetization process in anisotropic sheet, the product of the rotating matrix $\bar{\mu}_{iso}/\mu$ and $\bar{\mu}_{aniso}$ is used to give a rotational per unit loss per cycle of:[6]

$$P_R = \frac{B^2\pi}{T\delta}\left(\frac{1}{\mu_X} + \frac{1}{\mu_Y}\right)\sin\theta \qquad [6]$$

where T is the period of magnetization, and δ is the density.

The above equation is difficult to apply, consequently, it is far more convenient to develop relationships directly from Eq 2. If this expression is extended for the case of rapidly rotating magnetization, it becomes:

$$P_R = \frac{1}{T\delta}\int_o^T B_R H_R \sin\theta \, dt \qquad [7]$$

Note that the δ term converts to loss per unit mass rather than per unit volume in Eq 2. If orthogonal components of B and H are taken, as shown in Fig. 1(b), it can easily be shown that Eq 7 can be rewritten as:

$$P_R = \frac{1}{T\rho}\int_o^T \left(B_X H_Y - B_Y H_X\right) dt \qquad [8]$$

or

$$P_R = \frac{1}{T\rho}\int_o^T \left(H_X \frac{dB_X}{dt} - H_Y \frac{dB_Y}{dt}\right) \qquad [9]$$

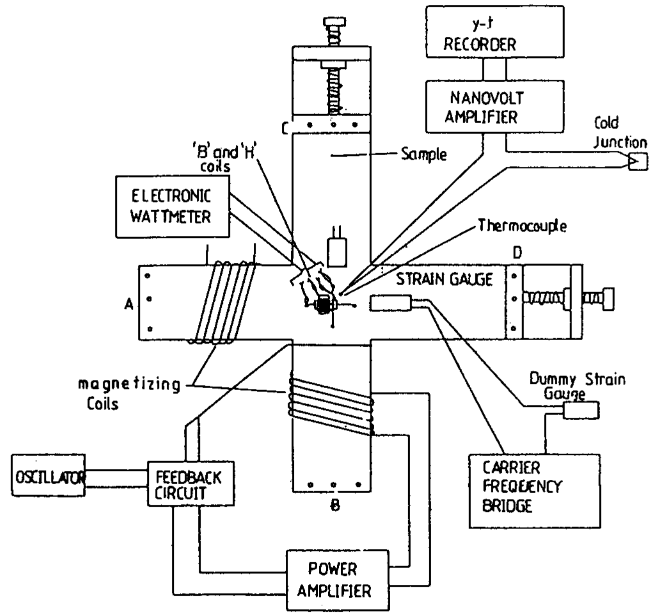

Fig. 4 System for rotational magnetization and loss measurement in a cross-shaped specimen of electrical steel.[8]

These equations represent the sum of the eddy current and the hysteresis loss and can be conveniently used for loss measurement, as will be shown in the next section. The angle between B_R and H_R at any instant in time is simply given by:

$$\theta = \arctan\left(\frac{b_X h_Y - b_Y h_X}{b_X h_X + b_Y h_Y}\right) \qquad [10]$$

where b_X, b_Y, h_X, and h_Y refer to instantaneous values of the X and Y components of rotational flux density and field, respectively.

3 Production and Measurement of Rotational Power Loss

It is very difficult to set up a pure rotating flux density in an anisotropic material. A pure rotating flux is regarded as one of fixed magnitude rotating at constant angular velocity in the plane of a sheet. It is generally attempted either to carry out measurements under pure rotating field or pure rotating flux density; both cannot occur simultaneously. Some representations of rotating flux are shown in Fig. 3. Figure 3(a) shows the magnitude and direction of flux density set up in isotropic mild steel and anisotropic grain-oriented silicon iron. The vectors show the magnitude and direction of the flux density after successive equal intervals in time through out the magnetizing cycle. In the case of the mild steel, pure rotational flux is easy to achieve, whereas the anisotropy of the grain-oriented steel causes the instantaneous flux to be high at the instant in time when it is directed along the easy direction. The locus of the flux density can be forced to be circular by applying suitable magnetizing conditions.

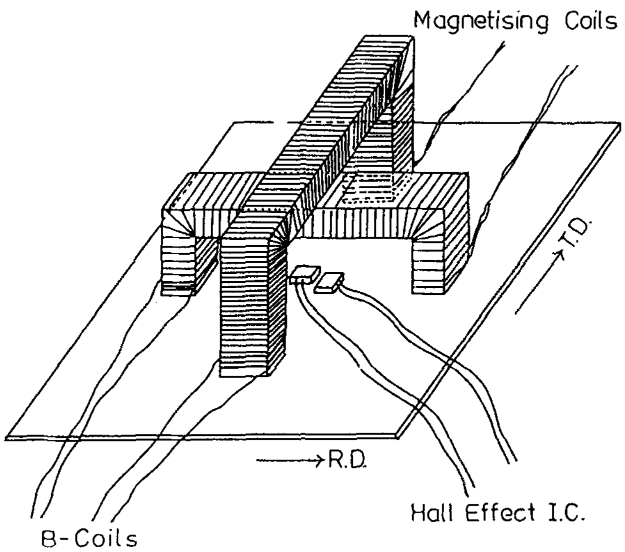

Fig. 5 Yoke system and field sensors for magnetization and field measurement in a square-shaped sample of electrical steel.

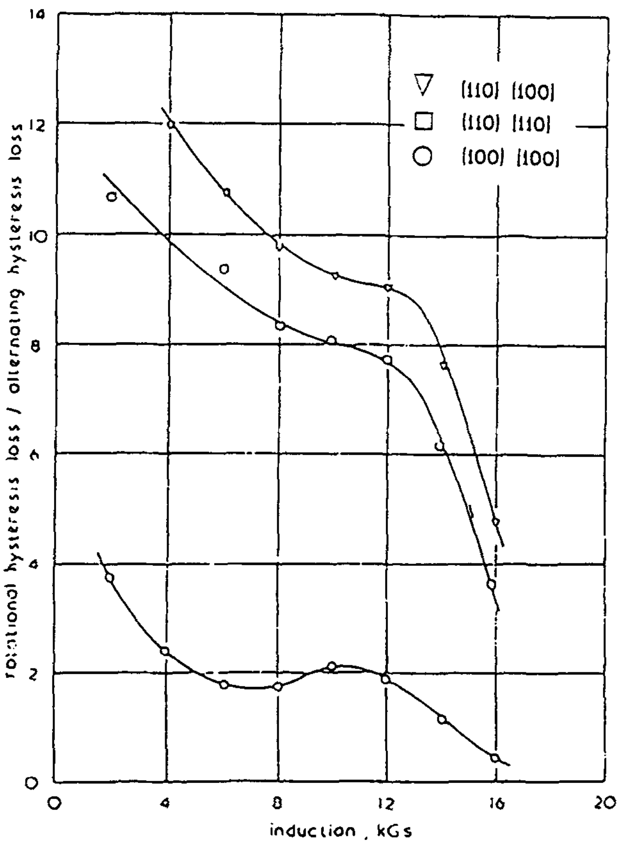

Fig. 7 Ratio of rotational power loss to alternating power loss in single crystals of silicon iron with **(a)** (110) [100], **(b)** (110) [110], **(c)** (100) [100] orientation.[3]

The pure rotating field is set up normally in a test specimen by magnetizing simultaneously in orthogonal directions by identical coils carrying ac currents equal in magnitude but 90° out of phase in time. By using suitable negative feedback techniques, these currents can be adjusted to produce pure rotational flux. In a transformer or rotating machine, laminations can be magnetized in a more complex form, such as that shown in Fig. 3(b).[7]

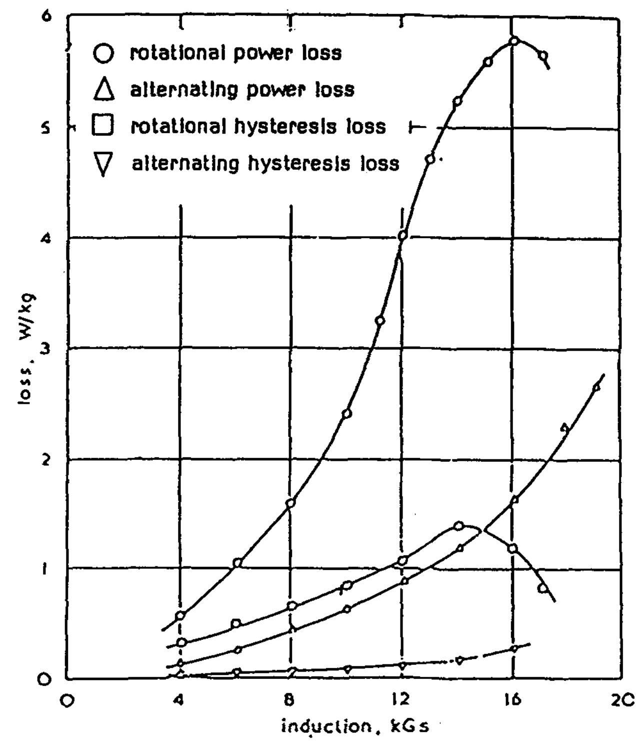

Fig. 6 Comparison between rotational power loss **(a)**, rotational hysteresis loss **(b)**, alternating power loss **(c)**, and alternating hysteresis loss in a sample of grain-oriented silicon iron.[3]

Table 1 Alternating and Rotational Power Loss in Various Materials and Their Ratios

Samples	Alternating power loss (P_{AC}), W/kg	Rotational power loss (P_R), W/kg	P_R/P_{AC}
Nonoriented 2.7% silicon iron	1.40	3.50	2.50
Nonoriented 1.2% silicon iron	1.23	4.00	3.25
Semiprocessed low-silicon iron	1.93	5.53	2.86
Four square 3.0% silicon iron (0.03 mm)	0.70	1.40	2.00
3.2% Goss-oriented silicon iron	0.46	1.84	3.90
Metglas 2605S-2	0.11	0.21	1.90
Powercore strip	0.12	0.130	1.05

Note: All values obtained at 1.0 T and 50 Hz.

Many methods have been used to set up rotational flux and measure rotational losses.[3,7-12] Figure 4 shows a measurement system in which a cross-shaped specimen is magnetized by orthogonal coils.[8] Yokes (not shown) are used for return flux paths, and the apparatus was designed to apply mechanical stress to the specimen during magnetic measurement. Only one magnetizing circuit is shown for clarity. Two loss measuring methods are indicated. One uses a thermocouple to sense the initial rate of rise of temperature in the region of the sample subjected to rotational flux to calculate the rotational loss. Ther-

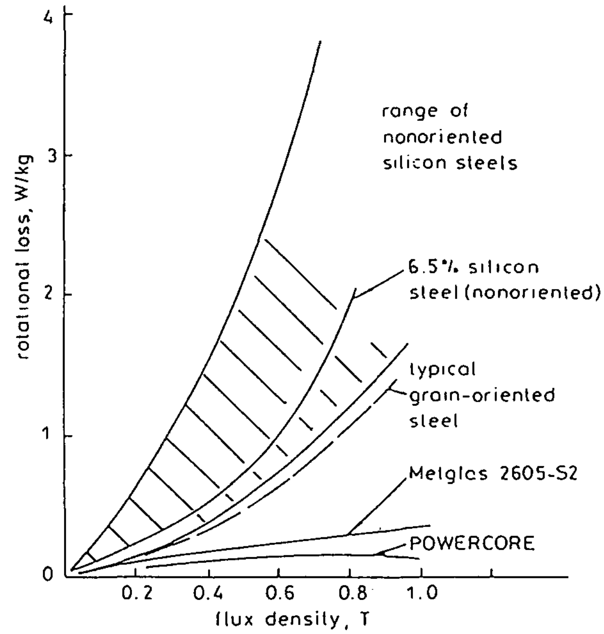

Fig. 8 Variation of rotational flux loss with flux density in various materials.[13]

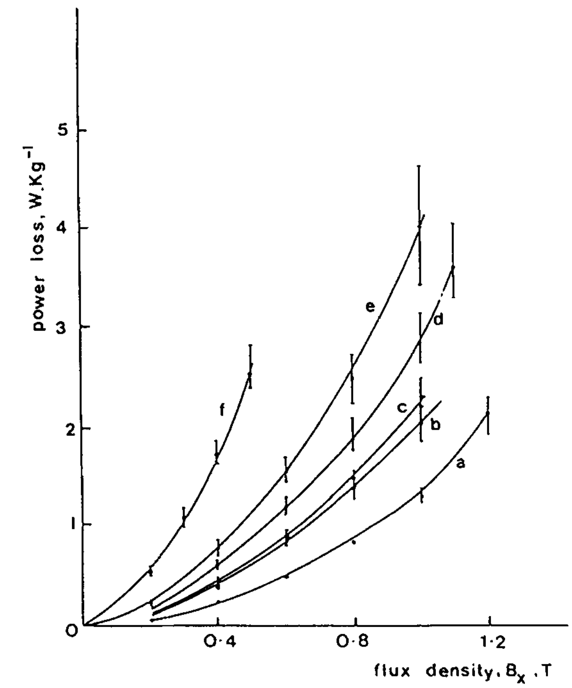

Fig. 9 Variation of rotational power loss with flux density with different degrees of rotational flux. (**a**) $B_Y = 0$. (**b**) $B_Y = 0.5\,B_X$. (**c**) $B_X = 0$. (**d**) $B_Y = 0.75\,B_X$. (**e**) $B_Y = B_X$. (**f**) $B_Y = 2B_X$.[10]

mistors are normally used for such measurements now. The second method makes use of B-coils wound through small holes drilled in the specimen and H-coils placed on its surface to instantaneous orthogonal components of B_R and H_R, respectively.

A system that avoids the need to drill holes for search coils and also produces more uniform magnetization is shown schematically in Fig. 5. The outputs of the B and H sensors are passed to an analogue-to-digital converter and then numerically processed according to Eq 9 to evaluate the rotational loss.

It has been suggested[11] that a magnetizing circuit with air gaps between the specimen and magnetizing yokes leads to more uniform magnetization. However, no consensus on the best type of magnetization system has been reached or on the type of loss measuring method that is most convenient to use.

4 Practical Rotational Loss Measurements

Figure 6 shows some early measurements of rotational loss in grain-oriented 3% silicon iron.[3] It can be seen that the total rotational loss is much higher than the alternating loss or the rotational hysteresis loss over the full flux density range. The peak and drop on the approach to saturation can be observed. Figure 7 shows the ratio of rotational to alternating hysteresis loss measured in three types of silicon iron single crystals.[3] The (100)[100] crystal yields values close to 2 (as predicted by Ref 5), but it should be noted that in the more anisotropic materials the ratio is much higher. The ratios of total rotational loss to alternating loss, both at 1.0 T and 50 Hz, are shown in Table 1 for a range of materials. The Goss-oriented steel has the highest value, as expected from Fig. 7, and the most isotropic materials have low values. The very low value for Powercore strip is unexpected and may be due to errors caused by inaccuracy in measuring rotational loss in such material.

Figure 8 shows the typical variations of rotational loss with flux density (50 Hz) in a range of materials.[13] In spite of the high ratio of rotational loss to alternating loss in grain-oriented steel, its absolute value is still less than that of more nonoriented silicon steels. The large range of values of the nonoriented steels should be noted, because it illustrates an area for possible improvement.

The effect of having a nonuniform magnitude of rotational flux is shown in Fig. 9.[10] The results show that the loss under ac magnetization along the rolling direction in this material is less than when magnetized along the transverse direction, *i.e.*, the material has some degree of anisotropy. Curve (**e**) shows the pure rotational loss characteristic, and it can be seen that varying the ratio of the magnitude of the major to minor axis flux density results in a wide variation in losses.

5 Rotational Flux in Rotating Machines and Transformers

The previous sections have given an indication of the nature and magnitude of rotational losses in electrical steels. Now its occurrence in laminated cores is considered. Rotational flux occurs in the so-called T-joints of three-limb, three-phase laminated transformer cores. In these regions, the flux needs to change its path at different times during the magnetizing cycle, because the three limbs are magnetized in sequence. The directional change is brought about by either flux transfer between

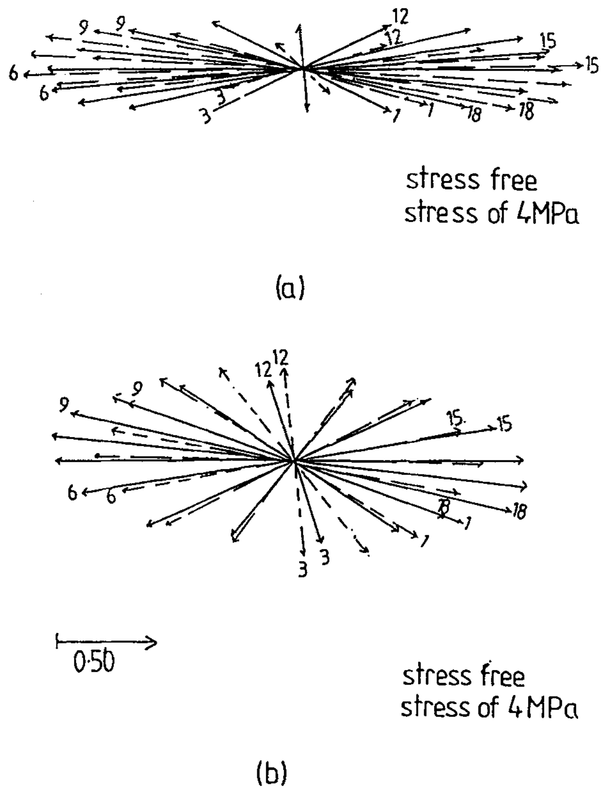

Fig. 10 Instantaneous fundamental components of flux density measured with and without the presence of a radial compressive stress in a stator lamination of an induction motor. (**a**) Behind slot. (**b**) Behind teeth.[15]

adjacent layers of laminations at the joints or by rotation in the plane of the lamination. The degree to which either of these mechanisms predominates will depend mainly on the T-joint design and the type of material used.

The ac rotating machine cores are subjected to rotating magnetic fields that are set up by currents in the phase windings. It has been known for some time[2] that various parts of stator cores of alternators and induction motors are subjected to large degrees of rotational flux in this way. In large stators, the core is also segmented, and this also controls the amount and location of the rotational flux.[14]

There are two ways of investigating rotational flux and losses in machines. The first, which has been used successfully for some time, is to place flux and temperature sensors at various parts of model laminated cores. This is tedious and creates a small disturbance to the model, but the characteristics of real materials and geometries are taken into account. Rotational losses and flux density can be measured locally within a core to an uncertainty, usually which is not greater than ± 3% using these techniques. The second approach is to use the finite-element method (FEM) to model a geometry and to calculate the field, flux density, and finally the losses. This method has been used successfully to model ideal cores, but it is still difficult to accurately take into account material anisotropy and to obtain accurate estimates of losses. Several obstacles must be overcome before finite-element methods can be used to accurately calculate rotational losses in machines.

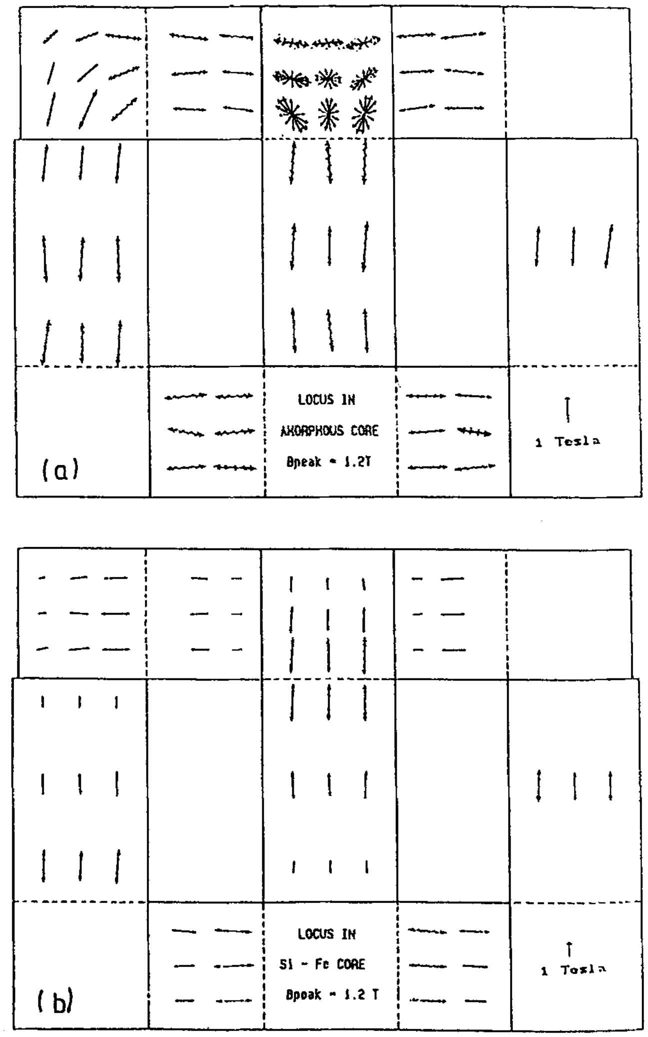

Fig. 11 Locus of localized fundamental component of flux density in model three-phase three-limb cores assembled from (**a**) amorphous ribbons and (**b**) grain-oriented silicon iron. Limb flux density of 1.2 T, 50 Hz in each case.

In both methods, it is necessary to estimate the rotational loss in localized regions where not only flux rotation occurs, but superimposed harmonics, normal flux, and other factors contribute to additional localized losses. When using the experimental method, care must be taken to avoid stress or poor assembly practice, but at the same time, it is sometimes useful to be able to intentionally introduce controlled stress to study the performance of a core when subjected to practical building constraints. Experimental measurements of the effect of radial stress on localized rotational flux in a stator core are shown in Fig. 10.[15] In each case, numbers 1 through 12 indicate the magnitude and direction of the flux after equal intervals in time during the magnetizing cycle.

6 Rotational Flux and Loss in Transformers

As stated in the last section, the amount and location of rotational flux in a transformer will depend on the T-joint geometry

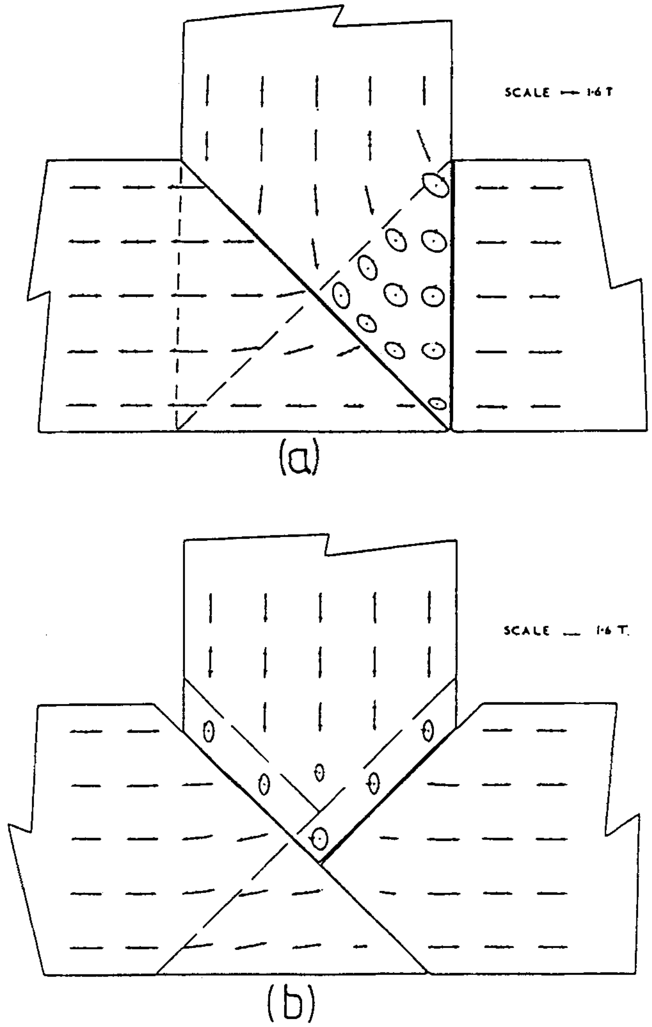

Fig. 12 Locus of 50-Hz components of localized flux density in the **(a)** 45 to 90° T-joint, and **(b)** 45° offset T-joint assembled from grain-oriented silicon iron.[16]

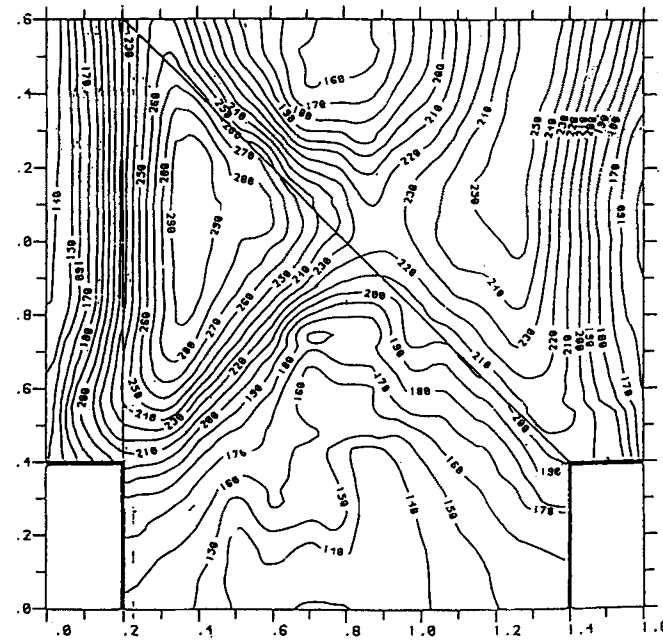

Fig. 13 Contours showing the variation of localized loss in the 45 to 90° T-joint showing peak due to rotational loss.[17]

Table 2 Estimate of Rotational Losses in Three-Phase Transformer Cores

	45 to 90° T-joints	45° Offset T-joints
Total joint volume, %	12.5	12.5
Volume carrying rotational flux, %	3.2	2.5
Mean joint loss, W/kg	1.75	1.57
Limb loss, W/kg	1.20	1.20
Mean loss in rotational flux area, W/kg	2.40	1.80
Total measured loss, W	160 (100%)	155 (100%)
Loss in T-joints, W	28 (17.5%)	24.5 (15.8%)
Rotational loss,	11 (7%)	7 (4.5%)

Note: 100 kVA, three-phase, three-limb transformers.

and on the magnetic properties of the core laminations. Figure 11 shows the rotational flux in two identical model cores measured under the same conditions, one assembled from Powercore strip and the other from grain-oriented silicon iron. Rotational flux is prominent in the T-joint of the amorphous material, but none is present in the silicon iron core showing the strong influence of the isotropic nature of the amorphous core. Because rotational loss in amorphous material is very low, the overall core performance is still good.

If the operating flux density or core geometry is changed, then the rotational flux will change. Figure 12 shows the rotational flux regions in 45 to 90° and 45° offset T-joint regions of grain-oriented silicon iron transformer cores operated at 1.5 T.[16] The regions of rotational flux are easily seen. The effect of the rotational flux on localized loss in the 45 to 90° T-joint is shown in Fig. 13.[17] A peak of over double the limb loss occurs where rotational flux occurs. In fact, high loss occurs due to high normal or interlamina flux in other regions also.

An estimate of the overall effect of rotational flux on the loss of transformers assembled with the 45 to 90° and the 45° offset T-joints has been made. Table 2 gives a comparison of the cores. In either case, the core volume carrying rotational flux is very small, and the rotational flux accounts for small proportions of the total loss. However, if the high rotational loss in grain-oriented steel could be reduced by 50%, it might be possible to reduce the total core loss by around 2%. This would be a worthwhile transformer loss saving, but it seems unlikely at present that the rotational loss of grain-oriented steel can be reduced by anything approaching this amount.

7 Rotational Flux and Loss in Rotational Machines

The rotating magnetic field in an ac rotating machine stator core causes rotational losses. Figure 14 shows how rotational

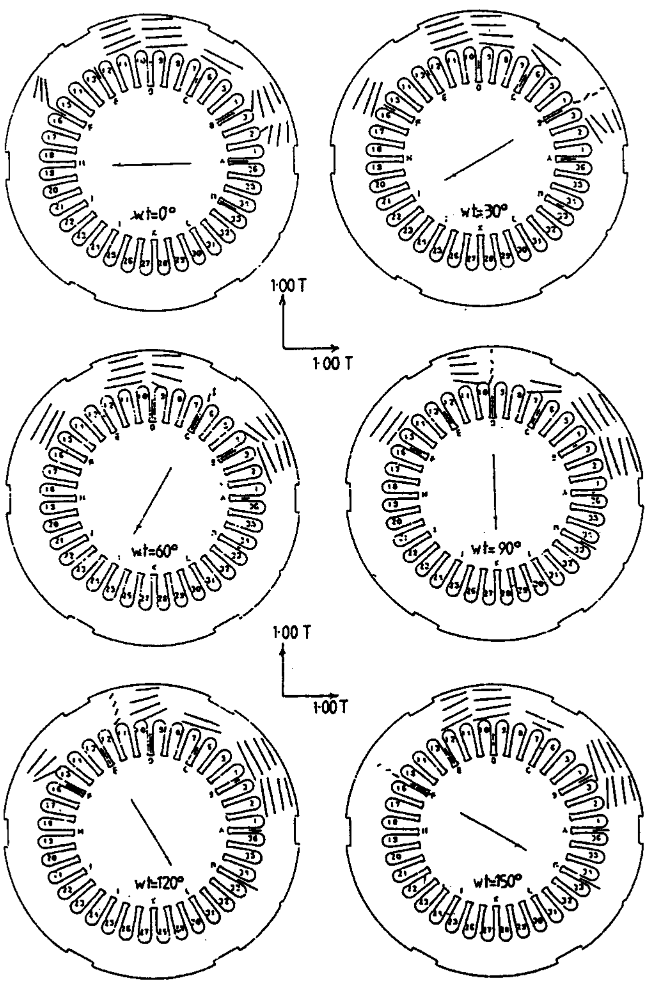

Fig. 14 Instantaneous localized variation of the fundamental component of flux density in an induction motor core assembled from nonoriented silicon iron at a core back flux density of 1.3 T and 50 Hz.

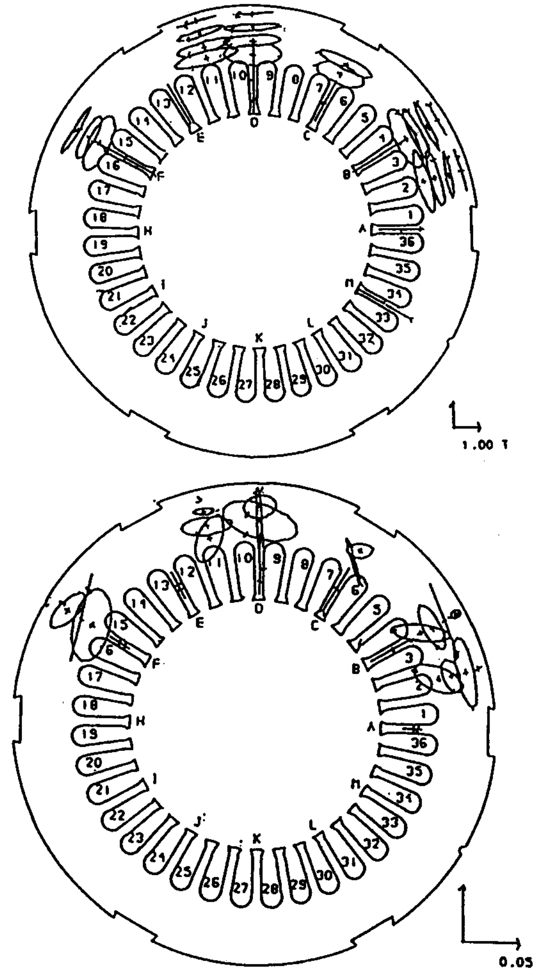

Fig. 15 Loci of the localized flux density in a three-phase induction motor stator core assembled from nonoriented silicon iron. **(a)** Fundamental (50 Hz). **(b)** Third harmonic (150 Hz) components of a core back flux density of 1.0 T.[17]

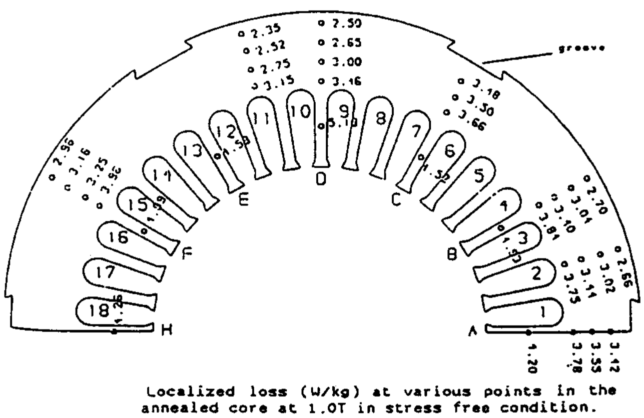

Fig. 16 Localized loss variation in the stator core whose localized flux distribution is shown in Fig. 15.[15]

flux originates in an induction motor stator core.[15] The instantaneous flux density magnitudes and directions are shown at six instants during the magnetizing cycle. The arrows represent the direction of the pole axis. Within the teeth and at the core back, the flux varies in magnitude, but does not change in direction. The locus of the flux density at several places in the same 3-kW induction motor stator core is illustrated in Fig. 15. Figure 15(a) shows the distribution of the first harmonic component (50 Hz) of flux density at various positions when the overall peak core flux density is 1.0 T. The high degree of rotational flux behind the teeth and slots is very noticeable. The core material in this case is a nonoriented silicon-free steel, but similar results are obtained from a wide variety of steels and over a wide range of core back flux densities. Figure 15(b) shows the distribution of the corresponding third harmonic component of flux density. This occurs in similar regions to those where the fundamental component of rotational flux occurs, but its magnitude is very much reduced (note the change of scale).

The loss in the same stator core is shown in Fig. 16. The figures refer to experimentally measured localized values of loss (W/kg). High losses occur in the teeth, as expected, and also in the regions subjected to the rotational flux. Other factors that control the magnitude of the localized loss are the position of the butt joints in this particular geometry and the location of the

Table 3 Estimate of Rotational Losses and the Effect of Reducing the Rotational Loss by 50%

	Volume, %	Mean iron loss, W/kg	Proportion of total loss %	W	Proportion of total loss when rotational loss is halved %	W
Core back carrying ac flux	28.3	2.63	22	17.6	30	17.6
Core back region carrying partial rotating flux	25.6	2.98	25.9	20.7	19.2	10.4
Core back region carrying rotation flux	27.6	3.64	29.5	23.6	19.8	11.7
Teeth	18.5	4.72	22.6	18.1	31	18.1
Total	100	3.37	100	80	100	58

Note: Three-phase 3-kW star-connected induction motor. Peak stator core back flux density = 1.0 T.

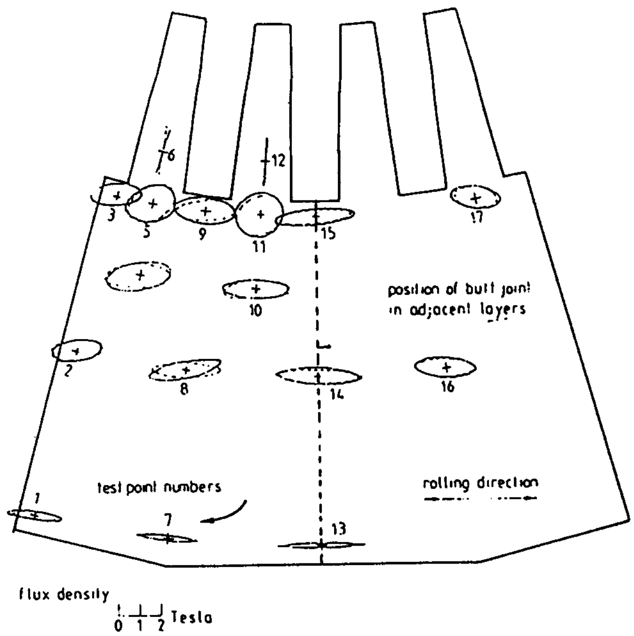

Fig. 17 Locus of localized fundamental components of magnetization in one segment of a three-phase turbogenerator stator core assembled from grain-oriented silicon iron.[14]

phase windings in the slots.[15] Discussion of these factors is beyond the scope of this article.

The results given here refer to a small three-phase, 415-V, 3-kW induction motor stator core, but similar distributions are obtained in larger machines such as segmented turbogenerator cores assembled from nonoriented or grain-oriented silicon iron.[14] Figure 17 shows the distributions of the fundamental component of flux density found in a segment of a model of a two-pole, 380MVA turbogenerator stator core with an outer core diameter of 1.1 m. In this case, the core back flux density was 1.5 T, and the material used is grain-oriented silicon iron. The dotted line loci at each point are the results taken at identical positions on different laminations showing the small effect on the results of material inhomogeneity on measurement errors.

Table 3 shows an attempt to estimate the contribution of rotational loss to the total core loss of the small induction motor considered earlier. The core volume is divided into regions carrying no rotational flux (*i.e.*, the teeth and the outer core back), some rotational flux, and where the flux is close to purely rotational. It can be seen that over 50% of the core volume is subjected to at least some rotational flux. Experimental values of measured localized loss are used to estimate the actual loss in each region. It can be seen that over 55% of the total loss of 80 W (watts) occurs where rotational flux predominates.

The final two columns in Table 3 give an estimate of the effect of using a steel with the same nominal loss under ac magnetization, but with half the rotational loss of the material actually used. Now the total loss has dropped by 28%, and the rotational loss represents 40% of the new core loss. Whether this is achievable remains to be seen. However, it is a goal worth aiming for, because the core losses in motors represent around 30% of all magnetic losses in electrical steels and they comprise around 7% of all motor losses, which consumes a sizable proportion of all generated electrical energy.

8 Conclusion

There is an increasing interest in the need for standardizing the measurement of rotational losses or even to introduce the property into material specifications. The amount of rotational losses occurring in transformers is only a small proportion of the total core loss, although a significant improvement in the rotational loss characteristics of grain-oriented silicon iron used in such apparatus would reduce overall losses by 2 to 3%. However, it is unlikely that such reduction can be obtained from grain-oriented steels.

Rotational losses in motors account for over 50% of their total core loss. Better understanding of the rotational magnetization process and loss mechanisms could lead to substantial energy savings in such devices. To achieve this improved, understanding it is necessary to measure rotational losses more accurately with the best techniques available and standardized measuring techniques should be developed.

References

1. IEC Standard 404-2 (1978).
2. R.J. Arnold, "Rotational Losses in Electrical Machines" CEGB Report RD/M/M86, Marchwood, UK (1971).
3. C.R. Boon and J.E. Thompson, *Proc. IEE, 112*(11), 2147-51 (1965).
4. R.D. Stratten and F.J. Young, *J.Appl. Phys., 33*(3), 1285-1287 (1962).
5. M. Kornetski and I. Lucas, *Z. Phys., 144*, 70-73 (1955).
6. W. Brix and K.A. Hempek, *J. Magn. Mag. Mat., 41*, 279-281 (1984).

7. A.J. Moses and B. Thomas, *IEEE Trans. Mag., MAG-9*(4), 651-654 (1973).

8. A. Basak and A.J. Moses, *Proc. IEE, 125*(2), 165-168 (1978).

9. Y, Ishibara and N. Takahasi, Mem. of Sch. of Eng. Okayama Univ., 14(1), 15-28 (1979).

10. M. Arabi and A.J. Moses, *J. Magn. Mag. Mat. 41*, 227-229 (1984).

11. W. Brix, K.A. Hempel and F.J. Schulte, *IEEE Trans. Mag., MAG-20*(5), 1708-1710 (1984).

12. W. Brix, K.A. Hempel and W. Schroeder, *IEEE Trans. Mag., MAG-18*(6), 1469-1471 (1982).

13. A.J. Moses, *IEE Proc. A, 137*(A), 5, 233-245 (1990).

14. A.J. Moses and G.S. Radley, *J. Magn. Mag. Mat. 19*, 60-62 (1980).

15. H. Rahmatizadeh, Ph.D. thesis, University of Wales (1990).

16. A.J. Moses and B. Thomas, *IEEE Trans. Mag. MAG-9*(4), 655-659 (1973).

17. R.S. Albir, Ph.D. thesis, University of Wales (1989).